RESEARCH ARTICLE | FEBRUARY 18 2022

Plasmonic photo-catalysis using a CdS–silver nanowire composite

Special Collection: 2022 Photonics & Optics

Ahmed T. Alanazi ; Sawsan Almohammed ; James H. Rice

AIP Advances 12, 025223 (2022)
https://doi.org/10.1063/5.0066216

Plasmonic photo-catalysis using a CdS–silver nanowire composite

Cite as: AIP Advances 12, 025223 (2022); doi: 10.1063/5.0066216
Submitted: 9 August 2021 • Accepted: 2 February 2022 •
Published Online: 18 February 2022

Ahmed T. Alanazi, Sawsan Almohammed, and James H. Rice[a]

AFFILIATIONS

School of Physics, University College Dublin, Belfield, Dublin 4, Ireland

[a]**Author to whom correspondence should be addressed:** James.rice@ucd.ie. **Present address:** School of Physics, University College Dublin, Belfield, Dublin, Ireland.

ABSTRACT

We examine the potential of cadmium sulfide when combined with plasmonic nanostructures to support photo-induced catalysis. Super-bandgap irradiation of a silver nanowire and cadmium sulfide composite for the probe molecule p-aminothiophenol (PATP) showed the formation of dimercaptoazobenzene (DMAB) from PATP. Our results demonstrate that cadmium sulfide can be used as an alternative material to semiconductors, such as titanium dioxide, for plasmonic photocatalysis applications.

Optical spectroscopy is widely applied as an analytical tool.[1–4] Modern fabrication techniques have enabled a wide range of materials to be made, including plasmon active nanomaterials.[5–14] Optical spectroscopy can be supported through plasmonics, enhancing the optical signal received by many orders of magnitude.[15–17] One example of this is surface-enhanced Raman spectroscopy (SERS), which enables ultrasensitive detection of a range of different analytes.[18–30] While the exact process by which SERS enhancement occurs is still under study, it is accepted that there are two different mechanisms, electromagnetic and chemical.[30–32] The electromagnetic enhancement mechanism is related to surface topography and the wavelength-dependent plasmonic properties of the plasmonic material.[30–32] Conduction electrons of the plasmonic nanostructure are stimulated by an incident electric field to create collective oscillations [localized surface plasmon resonances (LSPRs)], which enhance the Raman scattering intensities by factors of $\sim<10^{14}$.[31–33] The chemical enhancement arises from the chemical interaction (such as charge transfer processes) between the active substrate and analyte molecule. Chemical enhancement factors are typically $\sim10^{2}$.[31,32] In addition to its optical properties, LSPR excitation can contribute to control chemical reactions.[22–24,29,30] Such plasmonic catalyzed reactions enable milder conditions and alternative reaction pathways that are not possible via conventional, thermally activated transformations.[22] Combining plasmon-active metallic nanoparticles (NPs) and semiconducting materials has been shown to be an effective platform for both plasmonic catalysis and SERS.[22–24,29–32] For example, it has been shown that super-bandgap irradiation of peptide semiconductors with silver nanoparticle metamaterials enhances the SERS signal from a range of molecules.[24] The super-bandgap irradiation source possesses a wavelength greater than the bandgap of the semiconductor (e.g., UV light). Applying this irradiation source induced charge transfer, which facilitated a chemical enhancement that provides up to a tenfold increase in SERS intensity.[34] Additionally, the resonant excitation of surface plasmon resonance allows the nanoparticles to collect the energy of photons to form a highly enhanced electromagnetic field, and the energy stored in the plasmonic field can induce hot carriers in the metal. The plasmonic electromagnetic field and hot electrons can catalyze chemical reactions of reactants near the surface of the plasmonic metal nanoparticles.[30–32]

Here, we demonstrate that the use of single crystal cadmium sulfide (CdS) films when combined with plasmonic metal nanowires (NWs) is effective at supporting plasmonic catalysis and photo-induced surface-enhanced Raman spectroscopy. CdS is an n-type semiconductor material with a bandgap of ~2.4 eV (515 nm).[35] We show that the use of UV irradiation (l_{ex} = 266 nm) with a frequency higher in energy than the bandgap of CdS enables an increase in SERS intensity (~40-fold) along with the plasmon assisted catalysis of the starting reagent. Our results demonstrate that CdS can be used as an alternative material to semiconductors, such as titanium

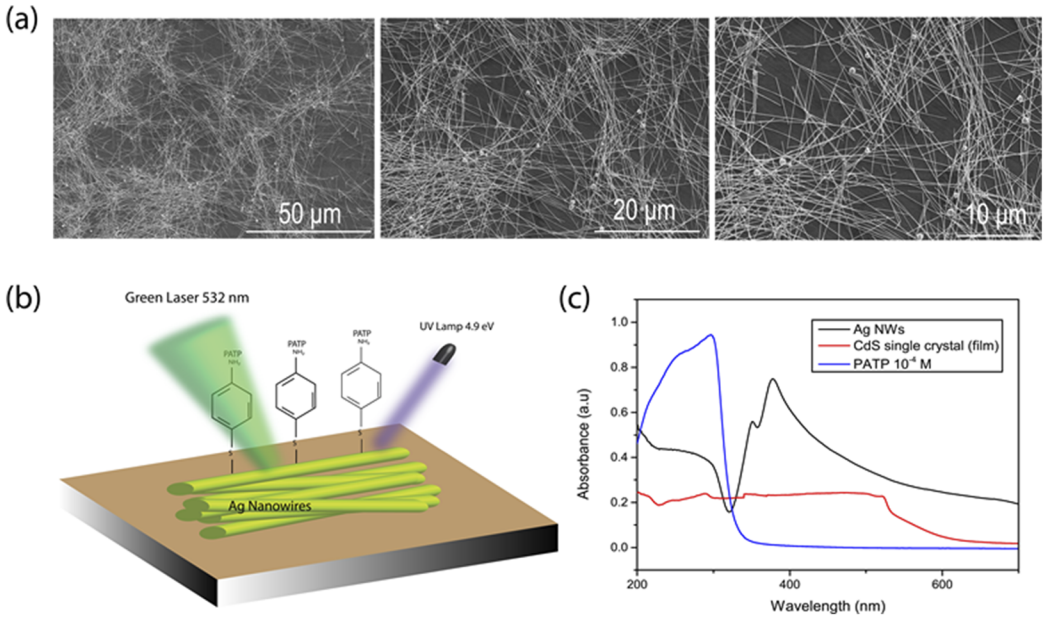

FIG. 1. (a) SEM images of silver nanowires (Ag NWs) on the semiconductor cadmium sulfide (CdS). (b) A schematic showing the nanowires on the CdS substrate. (c) Absorption spectra of the Ag NWs in solution prior to deposition. The absorption spectra of CdS and PATP are also shown.

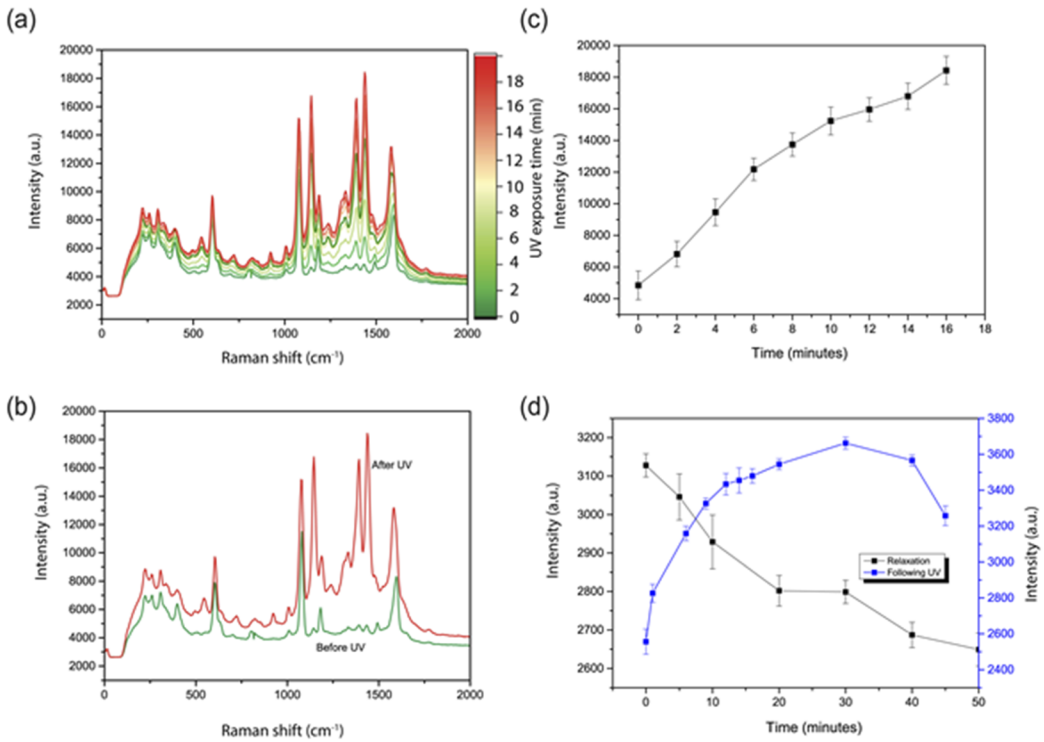

FIG. 2. SERS spectra of PATP on an Ag NW–CdS composite: (a) SERS measurements of PATP before and after UV irradiation (λ_{ex} = 266 nm) and (b) SERS spectra of PATP prior to UV irradiation and after 16 min of irradiation, showing the conversion of PATP to DMAP. (c) Plot of overall SERS intensity at 1432 cm^{-1} as a function of UV irradiation exposure over 16 min. (d) Plot of overall SERS signal intensity as a function of UV irradiation exposure time (blue dots). The relation of the overall SERS signal intensity (black dots) following the removal of UV irradiation, recorded over 60 min, is also shown.

dioxide, for photo-induced plasmon catalysis and SERS spectroscopy applications.

Silver nanowires (Ag NWs) were prepared on a CdS substrate through drop casting (as outlined in the supplementary material). The nanocomposite was then dried, and the probe molecule was added. The scanning electron microscopy (SEM) images of the resulting Ag NW–CdS composite (Fig. 1) show the presence of a dense network of nanowires present on the CdS surface. The optical absorption spectrum for CdS is shown along with the spectrum recorded for silver nanowires (Ag NWs). The spectrum for CdS shows an absorption band at 515 nm. Experimental values for the bulk hexagonal CdS optical bandgap are close to the value of 515 nm.[35] The absorption spectrum of Ag NWs shows two broad bands associated with transverse and longitudinal modes from the nanorod array, which are in line with literature reports (Fig. 1).[7,11,17]

Following the deposition of PATP on the composite, Raman measurements were undertaken following the exposure of the composite to UV light. The UV light source (4.9 eV) is of higher energy than the bandgap of CdS (2.4 eV).[35] This creates electron–hole pairs in the CdS substrate when under illumination. The SERS spectrum [Figs. 2(a) and 2(b)] before the application of super-bandgap excitation shows Raman bands with a_1 symmetry (at 1077 and 1190 cm^{-1}) and b_2 symmetry (1142, 1391, 1440, and 1573 cm^{-1})[22,30] assigned to PATP.[22,30] Following exposure to UV irradiation, new Raman bands appear [Figs. 2(a) and 2(b)]. Intense b_2 Raman bands at 1432, 1390, 1144, and 1076 cm^{-1} with 1088 and 1594 cm^{-1} a_1 Raman bands are formed. These Raman bands are assigned to arise from the dimerization of PATP forming DMAB.[22,30] Along with the formation of DMAB, a large change in the Raman signal is seen. The peak-to-peak band intensity for the vibrational mode at 1432 cm^{-1} increases ~40-fold following UV irradiation over 15 min. The formation of DMAP is approximately linear with time over this 15-min time-period [Fig. 2(c)]. Additional UV exposure time over 15 min causes a less pronounced increase in SER intensity as the rise in SERS intensity begins to plateau out

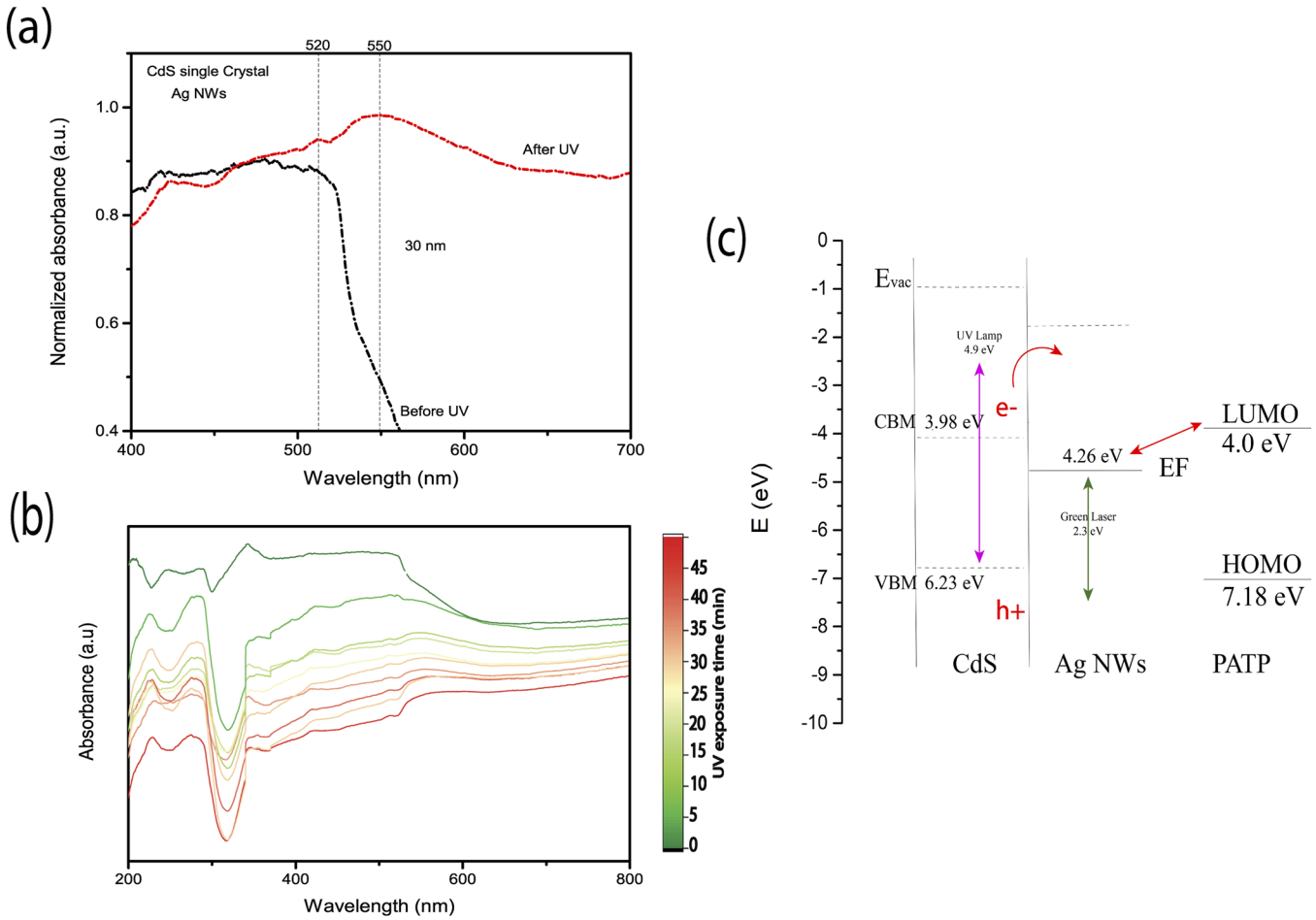

FIG. 3. (a) Absorption spectra of the Ag NW–CdS composite before and after UV irradiation. Gray dashed lines are guides to the eye, which outline peaks assigned to localized surface plasmons arising from longitudinal modes of Ag NWs. (b) Absorption spectra of the Ag NW–CdS composite following UV irradiation in 5-min increments. (c) An energy band diagram. The purple arrow shows the creation of electron–hole pairs in CdS following UV irradiation.

[Fig. 2(d), blue dots]. At UV irradiation times of greater than 30 min, the SERS intensity begins to drop. This is assigned to the onset of decomposition of the probe molecule. Following the removal of the UV irradiation, the relaxation of the SERS signal back to approximately original intensity was seen. Over the course of 45 min after the UV lamp was turned off [Fig. 2(d), black dots], the SERS intensity dropped back to near its starting intensity, demonstrating that the process is reversible.

The optical absorption spectrum of Ag NWs on CdS shows a strong absorption feature at ~520 nm, arising from the longitudinal mode of the nanowire. Following exposure to UV light (15 min), this feature becomes more pronounced and its peak red shifts by ~30–550 nm. This redshift potentially arises from an increase in Ag NW electron density following irradiation, which changes the reflective index of the nanowires.[32,36,37] We estimate the introduced electron density ($\Delta N/N$) on the Ag NWs following UV irradiation using the following equation:[38]

$$\frac{\Delta N}{N} = 2\Delta\lambda/\lambda_0, \tag{1}$$

where $\Delta\lambda$ is the wavelength shift (~30 nm) and λ_0 is the initial Ag NW plasmon band position (~520 nm). From Fig. 3(a), we calculate $\Delta N/N$ ~ 11%, which is higher than those reported for TiO_2 and metal NWs ($\Delta N/N$ ~ 4%).[33] The additional charges on the Ag NW (from photoexcited CdS) cause a redshift in the plasmon frequency, more in resonance with the excitation frequency. This results in an increase in SERS intensity. We note also that[39] CdS can support

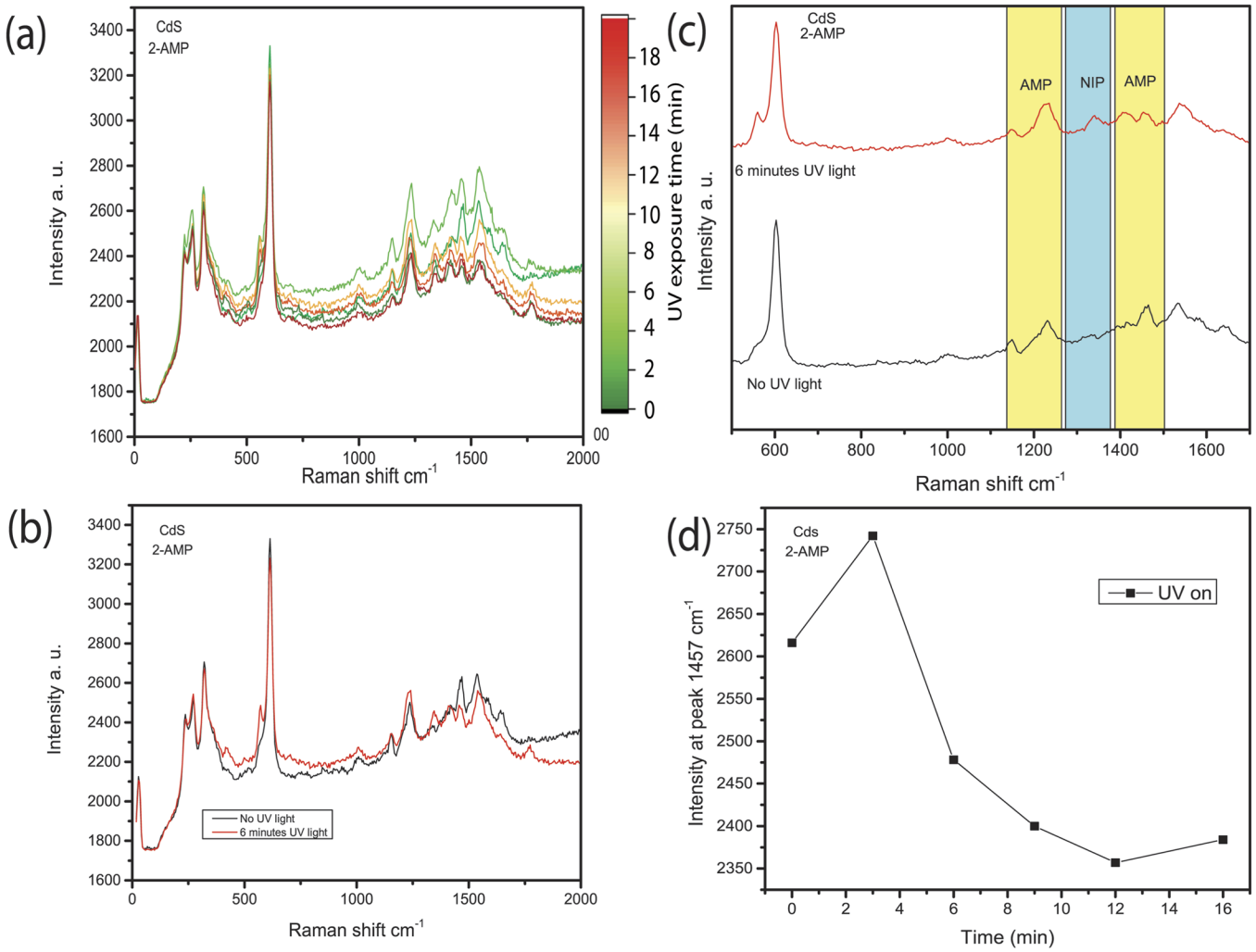

FIG. 4. SERS spectra of 2-AMP on an Ag NW–CdS composite: (a) SERS measurements of 2-AMP before and after UV irradiation (λ_{ex} = 266 nm) and (b) SERS spectra of 2-AMP prior to UV irradiation and after 6 min of irradiation, showing the conversion of 2-AMP to 2-NIB. (c) SERS spectra of 2-AMP before UV irradiation (black) after 6 min (red). (d) Plot of overall SERS signal intensity as a function of UV irradiation exposure time (black dots), recorded over 16 min.

SERS through a chemical enhancement mechanism. Studies have shown[39] that CdS nanoparticles support SERS. It is feasible that some chemical enhancement can, in principle, stem also from the semiconductor itself.

2-aminothiophenol (2-AMP) is a molecule that has been used to investigate plasmon catalysis reactions. As shown in Fig. 4, we performed UV irradiation of 2-AMP as before for PATP. The 2-AMP SERS spectra show peaks located at 1580 (C–C symmetric stretching mode), 1440 (C–H in-plane bending modes), 1390 (C–H in-plane bending modes), 1180 (C–H in-plane bending), 1145 (C–N stretching), and 1098 cm^{-1} (CS stretching).[40–45] Following 3 min of UV irradiation, the SERS intensity at 1457 cm^{-1} increased, and then, the SERS intensity begins to drop. Inspection of the spectra [Figs. 4(b) and 4(c)] shows that the NIP molecule has been formed from 2-AMP, indicating that the CdS–Ag NW substrate supported a catalytic reaction.

In summary, we examine the potential of cadmium sulfide when combined with plasmonic nanostructures to support plasmon catalysis. Super-bandgap irradiation of a silver nanowire and cadmium sulfide composite was shown to efficiently increase the SERS signal intensity. We demonstrate an increase in the peak-to-peak signal along with the catalysis of the starting molecule. Our results demonstrate that silver nanowires on cadmium sulfide can be used to support plasmon enhanced catalysis and SERS.

See the supplementary material for methods and materials and supporting measurements on the CdS substrate and probe molecules.

We acknowledge the Saudi Arabian government scholarship program for supporting this work, the Ministry of Education—Kingdom of Saudi Arabia (MOE, Ref. No. IR18131), and the Saudi Arabian Cultural Mission (SACM, Grant No. 01102019).

AUTHOR DECLARATIONS

Conflict of Interest

The authors have no conflict of interests in reporting on this work.

DATA AVAILABILITY

The data that support the findings of this study are available within the article and its supplementary material.

REFERENCES

[1] L. Rolinger, M. Rüdt, and J. Hubbuch, Anal. Bioanal. Chem. **412**, 2047 (2020).
[2] J. H. Na *et al.*, Appl. Phys. Lett. **86**, 083109 (2005).
[3] J. H. Rice, R. Aures, J.-P. Galaup, and S. Leach, Chem. Phys. **263**, 401 (2001).
[4] E. Kennedy, R. Al-Majmaie, M. Al-Rubeai, D. Zerulla, and J. H. Rice, RSC Adv. **3**, 13789 (2013).
[5] S. Kim, J. M. Kim, J. E. Park, and J. M. Nam, Adv. Mater. **30**, 1870320 (2018).
[6] J. H. Rice *et al.*, Physica E **21**, 546 (2004).
[7] S. Fedele, M. Hakami, A. Murphy, R. Pollard, and J. Rice, Appl. Phys. Lett. **108**, 053102 (2016).
[8] S. Almohammed *et al.*, RSC Adv. **6**, 41809 (2016).
[9] M. Fanti *et al.*, J. Chem. Phys. **116**, 7621 (2002).
[10] D. Kilinc *et al.*, Appl. Phys. Lett. **110**, 053702 (2017).
[11] S. Ferdele, B. Jose, R. Foster, T. E. Keyes, and J. H. Rice, Opt. Mater. **72**, 680 (2017).
[12] K. Ryan *et al.*, Sci. Technol. Adv. Mater. **18**, 172 (2017).
[13] R. M. Al-Shammari, M. Manzo, K. Gallo, J. H. Rice, and B. J. Rodriguez, J. Phys. Chem. C **121**, 6643 (2017).
[14] A. Fularz, S. Almohammed, and J. H. Rice, J. Appl. Phys. **128**, 213105 (2020).
[15] S. Damm *et al.*, Appl. Phys. Lett. **106**, 183109 (2015).
[16] F. Lordan *et al.*, Plasmonics **8**, 1567 (2013).
[17] S. Damm *et al.*, Plasmonics **9**, 1371 (2014).
[18] N. Al-Attar *et al.*, Chem. Phys. Lett. **535**, 146 (2012).
[19] D. McNamara *et al.*, Int. J. Refract. Met. Hard Mater. **52**, 114 (2015).
[20] M. Harsha Vardhan Reddy *et al.*, Phys. Chem. Chem. Phys. **16**, 4386 (2014).
[21] E. Kennedy, R. Al-Majmaie, M. Al-Rubeai, D. Zerulla, and J. H. Rice, J. Biophotonics **8**, 133 (2015).
[22] S. Almohammed, S. Tade Barwich, A. K. Mitchell, B. J. Rodriguez, and J. H. Rice, Nat. Commun. **10**, 2496 (2019).
[23] S. Almohammed, F. Zhang, B. J. Rodriguez, and J. H. Rice, J. Phys. Chem. Lett. **10**, 1878 (2019).
[24] S. Almohammed, S. Fedele, B. J. Rodriguez, and J. H. Rice, J. Raman Spectrosc. **48**, 1799 (2017).
[25] R. M. Al-Shammari *et al.*, ACS Omega **3**, 3165 (2018).
[26] A. Fularz, S. Almohammed, and J. H. Rice, ACS Appl. Nano Mater. **3**, 1666 (2020).
[27] S. Almohammed *et al.*, ACS Appl. Nano Mater. **2**, 5029 (2019).
[28] N. Alattar *et al.*, Appl. Opt. **57**, E184 (2018).
[29] S. Almohammed, B. J. Rodriguez, and J. H. Rice, Sens. Bio-Sens. Res. **24**, 100287 (2019).
[30] S. Almohammed *et al.*, ACS Appl. Mater. Interfaces **12**, 48874 (2020).
[31] P. A. Mosier-Boss, Nanomaterials **7**, 142 (2017).
[32] G. McNay, D. Eustace, W. E. Smith, K. Faulds, and D. Graham, Appl. Spectrosc. **65**, 825 (2011).
[33] S. Ben-Jaber *et al.*, Nat. Commun. **7**, 12189 (2016).
[34] J. Zhao *et al.*, Nanoscale **13**, 8707 (2021).
[35] R. Banerjee, R. Jayakrishnan, R. Banerjee, and P. Ayyub, J. Phys.: Condens. Matter **12**, 10647 (2000).
[36] M. Kahraman, E. R. Mullen, A. Korkmaz, and S. Wachsmann-Hogiu, Nanophotonics **6**, 831 (2017).
[37] S. Almohammed, F. Zhang, B. J. Rodriguez, and J. H. Rice, Sci. Rep. **8**, 3880 (2018).
[38] P. Mulvaney, J. Pérez-Juste, M. Giersig, L. M. Liz-Marzán, and C. Pecharromán, Plasmonics **1**, 61 (2006).
[39] Q. Liu *et al.*, Spectrochim. Acta, Part A **66**, 202 (2007).
[40] L.-B. Zhao *et al.*, Phys. Chem. Chem. Phys. **14**, 12919 (2012).
[41] R. Jiang *et al.*, J. Phys. Chem. C **120**, 16427–16436 (2016).
[42] M. Muniz-miranda, J. Anal. Bioanal. Tech. **6**, 286 (2015).
[43] A. Hernández-Gordillo *et al.*, J. Photochem. Photobiol., A **257**, 44–49 (2013).
[44] T. Aditya *et al.*, Chem. Commun. **51**, 9410–9431 (2015).
[45] A. A. Ismail *et al.*, J. Mol. Catal. A: Chem. **358**, 145–151 (2012).